# Artificial Atoms Can Do More Than Atoms: Deterministic Single Photon Subtraction from Arbitrary Light Fields

Jens Honer,[1] R. Löw,[2] Hendrik Weimer,[1,3,4] Tilman Pfau,[2] and Hans Peter Büchler[1]

[1]*Institute for Theoretical Physics III, University of Stuttgart, Stuttgart, Germany*
[2]*5. Physikalische Institut, University of Stuttgart, Stuttgart, Germany*
[3]*Physics Department, Harvard University, Cambridge, Massachusetts 02138, USA*
[4]*ITAMP, Harvard-Smithsonian Center for Astrophysics, Cambridge, Massachusetts 02138, USA*

We study the interplay of photons interacting with an artificial atom in the presence of a controlled dephasing. Such artificial atoms consisting of several independent scatterers can exhibit remarkable properties superior to single atoms with a prominent example being a superatom based on Rydberg blockade. We demonstrate that the induced dephasing allows for the controlled absorption of a single photon from an arbitrary incoming probe field. This unique tool in photon-matter interaction opens a way for building novel quantum devices, and several potential applications such as a single photon transistor, high fidelity $n$-photon counters, or the creation of nonclassical states of light by photon subtraction are presented.

PACS numbers: 42.50.Ct, 32.80.Ee, 42.50.Dv, 42.50.Ex

The prime model for our understanding of resonant light-matter interaction is based on two energy levels of a single atom coupled by a dipole moment to the electromagnetic radiation. On the other hand, artificial atoms [1–8], which are based on two states of a more complex quantum many body system, can exhibit properties superior to the conventional single atom. Here, we show that an artificial superatom made of a large number of scatterers under the influence of a blockade mechanism exhibits the extraordinary property to deterministically absorb a single photon of an arbitrary incoming light field. The main idea is based on an externally induced controlled dephasing for the excitations. This unique tool in photon-matter interaction opens a way for building novel quantum devices such as a single photon transistor, high fidelity $n$-photon counters, or for the creation of nonclassical states of light by photon subtraction [9–12].

One way to reduce the physics of a mesoscopic ensemble of $N$ scatterers to two relevant energy levels is to introduce a strong interaction between the excited states. Such a scenario is realized for an ensemble of atomic atoms driven resonantly into a Rydberg level giving rise to the so-called Rydberg blockade phenomena [2,13–17], and also for semiconductor quantum dots [4]. In these cases the excited state is the coherent superposition with a single excitation shared among the particles providing an enhanced coupling $\sim\sqrt{N}$ compared to an individual scatterer [18–20]. It is this strong coupling which features superatoms as ideal quantum information processor for photons [2,21–23], while many tools currently developed for single atom-photon coupling (see [24] and references therein) can be directly carried over. On the other hand, superatoms can exhibit phenomena that are superior to

conventional atoms, e.g., as a strongly directed single photon source [25–27].

Here, we show that an artificial superatom based on Rydberg blockade provides a high fidelity and saturable single photon absorber; i.e., for an arbitrary incoming probe field, a single photon is subtracted and a Rydberg excitation generated, while the remaining part of the probe field propagates through the medium. In contrast, for a single atom the limit to absorb a single photon with a probability higher than 50% is only achieved by stringent requirements on the pulse shape or arrival time: a well-controlled $\pi$ pulse and its analogue on the single photon level [28] can coherently excite a single atom, while stimulated Raman adiabatic passage (STIRAP) demands control on the arrival time of the probe field. The scheme presented here circumvents these restrictions and provides a unique tool for quantum information processing. We demonstrate applications of this setup for the design of a single photon transistor, a high fidelity $n$-photon detector, and the creation of nonclassical states of light by photon subtraction.

The main idea is based on the combination of enhanced light-matter coupling in the mesoscopic ensemble with a controlled dephasing between the atoms. More specifically, the superatom possesses $N - 1$ dark states in addition to the two bright states forming the two-level system; see Fig. 1. Using an external dephasing allows us to couple the collective excited state to these dark states and distribute the excited state population over all $N$ levels. As a consequence, one obtains an equal population of these states and the probability to absorb a single photon scales as $N/(N + 1)$; it reaches unity for the large number of scatterers involved. While this general method can be applied to arbitrary artificial atoms based on a blockade
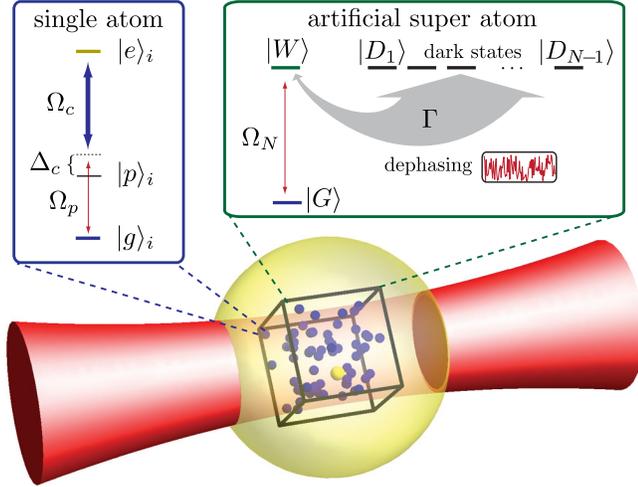
FIG. 1 (color online). Artificial superatom based on Rydberg atoms: for each atom the transition to the Rydberg state takes place via an intermediate $p$ level and a strong coupling laser with Rabi frequency $\Omega_c$ and detuning $\Delta_c$. Within the mode volume of the probe field with Rabi frequency $\Omega_p$, there are $N$ atoms within the collective blockade radius (yellow sphere) exceeding the cell size. The system gives rise to a superatom state $|W\rangle$ with a single Rydberg excitation shared among the particles with collective Rabi frequency $\Omega_N$. In addition, the system exhibits $N-1$ dark states $|D_j\rangle$, which are coupled to the superatom state by a controlled inhomogeneous dephasing with rate $\Gamma$.

mechanism, we will present the analysis for an ensemble of atoms laser driven into a Rydberg state. In addition, we point out that the presented scheme does not require a precise knowledge of the number of atoms in the trap.

The setup for the superatom consists of $N$ atoms confined in a small trap, which can be excited into a Rydberg state $|e\rangle_i$ through a two-photon transition: a strong laser field couples the Rydberg state $|e\rangle_i$ and the intermediate level $|p\rangle_i$ with Rabi frequency $\Omega_c$ and detuning $\Delta_c \gg \Omega_c$, while the transition from the ground state $|g\rangle_i$ to the intermediate $|p\rangle_i$ level is driven by the probe field with Rabi frequency $\Omega_p$; see Fig. 1. In the following, we assume near resonant light for this two-photon transition. The strong interaction between the Rydberg atoms gives rise to a collective blockade radius $r_B = (C_6/\hbar\sqrt{N}\Omega)^{1/6}$ with the two-photon Rabi frequency $\Omega = \Omega_c\Omega_p/4\Delta_c$ [16]. We are interested in the regime where all atoms are trapped within the Blockade radius. Then, only a single Rydberg excitation is possible and the relevant states of the $N$-body system are the state $|G\rangle$ with all atoms in the ground state and the excited states $|i\rangle$ with the $i$th atom excited to the Rydberg state. In addition, we require that the probe beam is strongly focused with a transverse mode area $A$ smaller than the size of the transverse trapping of the atomic system; see Fig. 1. With a characteristic size of the blockade radius in the range of 5 $\mu$m [16], these conditions can be well satisfied with current techniques for cold atomic gases.

In the "frozen" Rydberg regime, the system reduces to a superatom with the ground state $|G\rangle$ and the excited $W$ state $|W\rangle = \sum_i |i\rangle/\sqrt{N}$ accounting for the coherent superposition of a single Rydberg excitation. The coherent dynamics is given by the Hamiltonian

$$H = \frac{\hbar\Omega_N}{2}[|W\rangle\langle G| + |G\rangle\langle W|] \quad (1)$$

describing the coupling between the two bright states with the collective Rabi frequency $\Omega_N = \sqrt{N}\Omega$.

Several mechanisms can lead to decoherence and dephasing of the superatom. We distinguish between homogeneous and inhomogeneous decoherence: the first one acts on all atoms in the same way, e.g., fluctuations in the phase of the driving lasers, and leads to the dephasing of the superatom in analogy to a single atom. In turn, the inhomogeneous dephasing will influence each atom individually and gives rise to a fundamental difference between a single atom and the superatom [29,30].

An ideal inhomogeneous dephasing acting on each Rydberg atom can be microscopically designed by an ac Stark shift $\Delta_i(t)$ of the Rydberg level by a speckle light field with short range correlations in space as well as in time [31]; i.e., the detuning exhibits a spatial correlation $\xi$ comparable to the interparticle distance and a temporal correlation $\tau$ shorter than the collective Rabi frequency. Then, the random distribution of the atoms in the frozen Rydberg regime gives rise to the Hamiltonian accounting for the noise term

$$H_{\text{noise}} = \sum_i \Delta_i(t)|i\rangle\langle i| \quad (2)$$

with the correlations between the different detunings $\langle\Delta_i(t)\Delta_j)(t')\rangle = \Gamma\delta_{ij}\delta(t-t')$. This term in the Hamiltonian couples the excited bright state $|W\rangle$ with the additional dark states $|D_j\rangle$. Note that an alternative microscopic source for inhomogeneous dephasing is obtained by the combination of a pulsed coupling laser with optical lattices. In addition, the motion of the atoms beyond the frozen Rydberg approximation is an intrinsic mechanism leading to inhomogeneous dephasing with $\Delta_i \approx \hbar\mathbf{k}\mathbf{v}_i$ [29]; here, $\mathbf{k}$ is the wave vector of the beam and $\mathbf{v}_i$ the velocity of the atom.

Then, the Lindblad master equation for the two bright states and the $N-1$ dark states becomes

$$\partial_t\rho = -\frac{i}{\hbar}[H,\rho] + \Gamma\sum_i^N(2c_i\rho c_i^\dagger - c_i^\dagger c_i\rho - \rho c_i^\dagger c_i) \quad (3)$$

with the jump operators $c_i = |i\rangle\langle i|$. The dephasing $\Gamma$ gives rise to an exponential decay of the coherences in the system, and the stationary solution for the density matrix reduces to

$$\rho = \frac{1}{N+1}\left(|G\rangle\langle G| + |W\rangle\langle W| + \sum_{j}^{N-1}|D_j\rangle\langle D_j|\right). \quad (4)$$

The fidelity to absorb a photon $f = 1 - \text{Tr}(\rho|G\rangle\langle G|) = N/(N+1)$ is strongly enhanced for large particle numbers and eventually approaches unity for $N \gg 1$. In contrast, for a single atom, this reduces to the well-known fundamental limit that on average we can only absorb a photon with probability $f = 1/2$. The full dynamics of the system can be obtained by a straightforward time integration of the master equation; see Fig. 2. For small dephasing $\Gamma < \Omega_N$ the system still exhibits Rabi oscillations, which eventually are damped out with the effective decay rate $\Gamma_{\text{eff}} = \Gamma$, while for increasing dephasing $\Gamma$ the system turns over-damped with $\Gamma_{\text{eff}} \sim \Omega_N^2/\Gamma$. The shortest time for equilibration is achieved at the crossover from the underdamped to the overdamped regime.

The validity for the setup to work for a probe pulse containing a few photons requires that a single photon is absorbed within the coherence time $\tau$ of the probe pulse, i.e., $\Gamma_{\text{eff}}\tau > 1$. Using the single photon Rabi frequency this condition reduces to optical thick media $\kappa > 1$ with

$$\kappa = 2\pi N \frac{d^2}{\hbar c A} \frac{\omega_p}{2\Gamma} \frac{\Omega_c^2}{4\Delta_c^2} = \frac{\Omega_c^2}{8\Delta^2}\frac{\gamma_p}{\Gamma}\kappa_p < \kappa_p, \quad (5)$$

the transverse mode area $A$, the dipole transition moment $d$, and the frequency of the probe field $\omega_p$. Here, $\kappa_p = 6\pi\lambda^2 N/A$ denotes the resonant optical thickness for the $|g\rangle_i \rightarrow |p\rangle_i$ transition. The last inequality is required as the spontaneous emission from the intermediate state has to be smaller than the dephasing of the Rydberg level. In turn, the full absorption has to take place on a time scale shorter than the spontaneous emission from the Rydberg level. These conditions are naturally satisfied for cold Rydberg gases: The resonant optical thickness $\kappa_p$ for a Rb Bose-Einstein condensate with $N = 10^3$ in a tight trap with frequency 1 kHz and Thomas Fermi radius $r_{\text{TF}} = 1.0\,\mu\text{m}$ reduces to $\sim 350$. Consequently, there is a large regime to adjust the detuning $\Delta$ and suppress losses from the intermediate state, i.e., $8\Gamma\Delta^2/(\Omega_c^2\gamma_p) \sim 10\text{--}30$, which provides a large optical thickness $\kappa \gtrsim 10$.

In combination with a robust detection scheme of the Rydberg excitation, the setup gives rise to a saturable single photon detector with near unity fidelity. Here, we envisage the detection of the Rydberg excitation via the combination of electromagnetic induced transparency (EIT) and Rydberg blockade [32,33]. The system is probed by a weak detection beam satisfying the EIT condition; i.e., its frequency is shifted by $\Omega_c^2/4\Delta_c$ compared to the probe field. Then, the detection beam passes through the cell without any phase shift if all atoms are in the ground state. However, as soon as a single Rydberg state is excited, the EIT condition is violated and the detection beam acquires a phase shift due to the real part in the dielectric response function [34]. The subsequent measurement of the phase shift via a homodyne detection provides a perfect single photon detector. In gate operation language, the setup acts as a classical single photon transistor: a single photon in the probe beam switches several photons in the homodyne detector.

Combining several single photon detectors into a chain of individually addressable cells then opens the unique possibility for a high fidelity $k$-photon detector; see Fig. 3: each cell absorbs only a single photon, while the probe beam reduced by a photon propagates to the next



FIG. 2 (color online).   Time evolution. The probability $\rho_{gg}$ for the atomic system to remain in the ground state decays exponentially with the rate $\Gamma_{\text{eff}}$ to the final value $1/(N+1)$. The numerical integration is performed for $N = 9$ in the overdamped regime for $\Gamma = 7\Omega_N$ (dashed red line), as well as in the underdamped regime with $\Gamma = \Omega_N$ (solid green line), and in the crossover $\Omega_N = 3\Gamma$ (dash-dotted blue line). The inset shows the dependence of the effective damping rate $\Gamma_{\text{eff}}$ from the collective Rabi frequency $\Omega_N$, with $\Gamma_{\text{eff}} = \Gamma/2$ for weak dephasing, while the crossover from the under- to overdamped regime appears at $\Omega_n \sim 3\Gamma$, the damping rate scales as $\Gamma_{\text{eff}} \sim 4\Omega_N^2/\Gamma$.



FIG. 3 (color online).   Setup for a high fidelity $k$-photon detector. (a) Illustration of the incoming probe field with three photons on a chain of several cells, each containing a deterministic single photon absorber. Each cell absorbs exactly one photon, while the remaining beam propagates to the next cell. (b) In the first three cells exactly one photon is absorbed and an atom is excited to the Rydberg state, which in turn is subsequently detected: the position of the last Rydberg excitation provides the number of photons within the beam.

detector. The subsequent measurement of the Rydberg excitation for each cell provides the deterministic detection of the number of photons in the probe field.

Finally, the subtraction of photons from a squeezed vacuum field has extensively been discussed for the creation of nonclassical states of light such as cat states [9–12]. A major drawback of these schemes is a low probability for the reduction of the incoming beam by a single photon. Here, our scheme provides an advantage as a photon is subtracted, whenever a photon is present in the squeezed vacuum. The influence on the incoming probe field of the single photon absorption is well accounted for in a master equation approach. The single photon detector is described by two states: $|G\rangle$ for the atoms in the ground state and $|E\rangle$ for the state of the cell with a single Rydberg excitation detected. Then, the master equation describing the dynamics of the photon absorption and detection reduces to

$$\partial_t \rho = \Gamma_{\text{eff}}(2c\rho c^\dagger - c^\dagger c\rho - \rho c^\dagger c), \qquad (6)$$

where the jump operator $c = a|E\rangle\langle G|$ contains the photon annihilation operator $a$ and describes the transition to the state with a photon detected, while $\Gamma_{\text{eff}}$ accounts for the time scale for the single photon absorption; see Fig. 2. Note that the jump operator satisfies $c^2 = 0$ corresponding to the fact that a single photon saturates the absorber. The master equation can be analytically solved for an initial state $\rho = |G\rangle\langle G| \otimes \rho_{\text{inc}}$ with $\rho_{\text{inc}} = \sum_{nm}\rho_{nm}|n\rangle\langle m|$ the density matrix for the incoming probe field. The absorption of the photon takes place on the time scale $\Gamma_{\text{eff}}$, and for $t \gg 1/\Gamma_{\text{eff}}$ the density matrix approaches the stationary solution

$$\rho \rightarrow p_{\text{vac}}|G\rangle\langle G| \otimes \rho_{\text{vac}} + (1 - p_{\text{vac}})|E\rangle\langle E| \otimes \rho_{\text{out}}, \quad (7)$$

with $p_{\text{vac}}$ the probability for the initial photon state to be in the vacuum $\rho_{\text{vac}} = |0\rangle\langle 0|$. The density matrix describing the outgoing photon field takes the form

$$\rho_{\text{out}} = \frac{1}{1 - p_{\text{vac}}} \sum_{n,m=1} \frac{2}{n+m} \sqrt{nm}\rho_{nm}|n-1\rangle\langle m-1|. \qquad (8)$$

The Wigner function for this density matrix with an incoming squeezed state is shown in Fig. 4 and exhibits the characteristic feature of a nonclassical state of light with negative values. Note that this state is different from the photon subtracted state in the context for the generation of photonic ''cat'' states [9–12], but shows large overlap with those, and consequently also with a photonic cat state. With probability $p_{\text{vac}}$ no photon is present in the incoming beam, and the outgoing beam remains in the vacuum state $\rho_{\text{vac}} = |0\rangle\langle 0|$, while with probability $1 - p_{\text{vac}}$ a photon is absorbed from the incoming beam. Note that this probability represents a fundamental limit on the fidelity to generate nonclassical states of light by single photon subtraction.

To summarize, we have identified a novel feature of artificial atoms based on a strong excited state blockade,
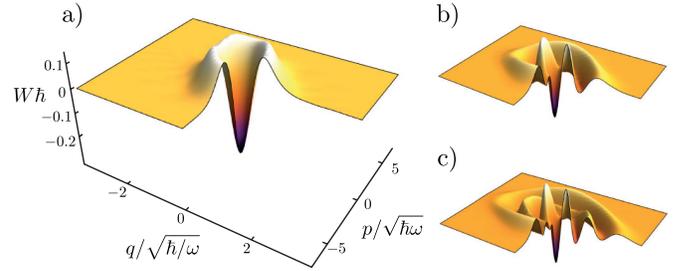


FIG. 4 (color online). Nonclassical states of light. (a) Wigner function of the outgoing photon state after the deterministic absorption of a photon within the cell. The incoming state is characterized by a coherent state ($\alpha = 0$) with subsequent amplitude squeezing ($w = 0.6$). The overlap between this state and a photon subtracted squeezed state ($w = 0.6$) discussed in [10] is 0.92. In addition, the Wigner function for the deterministic 3-photon absorption (b) as well as 5-photon absorption (c) are shown.

namely, their ability to act as a saturable deterministic single photon absorber when subjected to inhomogeneous dephasing. This goes beyond the known collective enhancement of their coupling to light fields and their ability to emit single photons in a directed fashion and provides a strong motivation to realize quantum devices based on an excited state blockade in a scalable arrangement.

[1]  P. Michler et al., Science **290**, 2282 (2000).
[2]  M. D. Lukin et al., Phys. Rev. Lett. **87**, 037901 (2001).
[3]  V. Vuletic, Nature Phys. **2**, 801 (2006).
[4]  A. J. Shields, Nat. Photon. **1**, 215 (2007).
[5]  D. I. Schuster et al., Nature (London) **445**, 515 (2007).
[6]  R. Schoelkopf and S. Girvin, Nature (London) **451**, 664 (2008).
[7]  J. Hwang et al., Nature (London) **460**, 76 (2009).
[8]  P. Neumann et al., Science **329**, 542 (2010).
[9]  B. Yurke, W. Schleich, and D. F. Walls, Phys. Rev. A **42**, 1703 (1990).
[10]  A. Ourjoumtsev, R. Tualle-Brouri, J. Laurat, and P. Grangier, Science **312**, 83 (2006).
[11]  J. S. Neergaard-Nielsen, B. M. Nielsen, C. Hettich, K. Mølmer, and E. S. Polzik, Phys. Rev. Lett. **97**, 083604 (2006).
[12]  V. Parigi, A. Zavatta, M. Kim, and M. Bellini, Science **317**, 1890 (2007).

[13] K. Singer, M. Reetz-Lamour, T. Amthor, L. G. Marcassa, and M. Weidemüller, Phys. Rev. Lett. **93**, 163001 (2004).

[14] D. Tong *et al.*, Phys. Rev. Lett. **93**, 063001 (2004).

[15] T. Vogt *et al.*, Phys. Rev. Lett. **97**, 083003 (2006).

[16] R. Heidemann *et al.*, Phys. Rev. Lett. **99**, 163601 (2007).

[17] M. Saffman, T. G. Walker, and K. Mølmer, Rev. Mod. Phys. **82**, 2313 (2010).

[18] Y. Colombe *et al.*, Nature (London) **450**, 272 (2007).

[19] A. Gaetan *et al.*, Nature Phys. **5**, 115 (2009).

[20] J. D. Pritchard *et al.*, Phys. Rev. Lett. **105**, 193603 (2010).

[21] B. Julsgaard, J. Sherson, J. I. Cirac, J. Fiurasek, and E. S. Polzik, Nature (London) **432**, 482 (2004).

[22] M. D. Eisaman *et al.*, Nature (London) **438**, 837 (2005).

[23] T. Chaneliere *et al.*, Nature (London) **438**, 833 (2005).

[24] N. Piro *et al.*, Nature Phys. **7**, 17 (2011).

[25] D. Porras and J. I. Cirac, Phys. Rev. A **78**, 053816 (2008).

[26] M. Saffman and T. G. Walker, Phys. Rev. A **66**, 065403 (2002).

[27] D. Felinto *et al.*, Nature Phys. **2**, 844 (2006).

[28] M. Stobińska, G. Alber, and G. Leuchs, Europhys. Lett. **86**, 14 007 (2009).

[29] J. V. Hernndez and F. Robicheaux, J. Phys. B **41**, 195301 (2008).

[30] Z. Kurucz, J. H. Wesenberg, and K. Mølmer, Phys. Rev. A **83**, 053852 (2011).

[31] J. Billy *et al.*, Nature (London) **453**, 891 (2008).

[32] M. Müller, I. Lesanovsky, H. Weimer, H. P. Büchler, and P. Zoller, Phys. Rev. Lett. **102**, 170502 (2009).

[33] M. Saffman and K. Mølmer, Phys. Rev. Lett. **102**, 240502 (2009).

[34] M. Fleischhauer, A. Imamoglu, and J. P. Marangos, Rev. Mod. Phys. **77**, 633 (2005).